THE JOURNAL OF BIOLOGICAL CHEMISTRY
Vol. 275, No. 36, Issue of September 8, pp. 27874–27882, 2000

Printed in U.S.A.

Induction of Vascular Endothelial Growth Factor in Human Astrocytes by Lead

INVOLVEMENT OF A PROTEIN KINASE C/ACTIVATOR PROTEIN-1 COMPLEX-DEPENDENT AND HYPOXIA-INDUCIBLE FACTOR 1-INDEPENDENT SIGNALING PATHWAY*

Received for publication, March 15, 2000, and in revised form, June 5, 2000
Published, JBC Papers in Press, July 5, 2000, DOI 10.1074/jbc.M002185200

Mir Ahamed Hossain‡§¶, Christopher M. L. Bouton§‖, Jonathan Pevsner§‖, and John Laterra‡§‖**

*From the Departments of ‡Neurology, ‖Neuroscience, and **Oncology, The Johns Hopkins University School of Medicine and §The Kennedy Krieger Research Institute, Baltimore, Maryland 21205*

The mechanism(s) underlying lead neurotoxicity are not fully elucidated. cDNA expression microarray analysis identified lead-sensitive genes in immortalized human fetal astrocytes (SV-FHA). Of the represented genes expressed, vascular endothelial growth factor (VEGF) was one of the most sensitive. Lead induced VEGF mRNA 3-fold and VEGF protein ~2-fold with maximum mRNA induction following incubation with 10 μM lead acetate for 24 h. Phorbol 12-myristate 13-acetate (PMA), a potent protein kinase C (PKC) activator, increased VEGF mRNA 2-fold and PKC inhibition by GF-109203 completely blocked VEGF induction by lead. Expression of dominant-negative PKC-ϵ, but not PKC-α, completely inhibited VEGF mRNA induction by lead. Lead activated the transcription factor AP-1 and increased AP-1-dependent luciferase expression >2-fold. Transfection of cells with a c-*jun* dominant-negative effectively inhibited both AP-1 activation and VEGF mRNA induction by lead. Hypoxia-inducible factor 1 (HIF-1) activity in SV-FHAs was moderately increased by lead (86%) and PMA (96%). Pretreatment with GF-109203 completely inhibited these effects of lead and PMA. However, lead did not alter HIF-1-dependent luciferase expression and a HIF-1α dominant-negative had no effects on the induction of VEGF mRNA by lead. These findings indicate that lead induces VEGF expression in SV-FHAs via a PKC/AP-1-dependent and HIF-1-independent signaling pathway.

Lead toxicity has been identified as the most important global environmental health hazard because of its prevalence in the environment and its potential to cause long lasting learning deficits and behavioral abnormalities particularly in children (1–5). Acute neonatal exposure leads to cerebral-microvascular pathology including blood-brain barrier dysfunction, cerebellar hemorrhage, and cerebral edema (6–8). The mechanisms leading to these diverse manifestations of lead toxicity are mostly unknown.

The biochemical and molecular mechanism(s) of action of lead neurotoxicity have not yet been fully elucidated. Several studies have shown, however, that calcium-dependent events are potential intracellular targets of lead (9, 10). Lead is reported to alter a number of calcium-mediated cellular processes including calcium channels and second messenger systems. Lead is a potent blocker of calcium channels, activates calmodulin with higher affinity than calcium (Ca^{2+}), and most importantly picomolar concentrations can substitute for Ca^{2+} in activating protein kinase C (PKC)[1] (11–13). PKC is a phospholipid-dependent diacylglycerol-activated serine/threonine protein kinase consisting of a multigene family of closely related, but distinct, isoenzymes (14, 15). Activation of PKC by lead results in the induction of the immediate-early-response genes c-*fos*, c-*jun,* and *erg*-1 (16, 17). Homodimerization (Jun family proteins) and heterodimerization (Jun and Fos family members) of these early response gene proteins form the activator protein-1 complex (AP-1) that mediates its subsequent effects on gene transcription (18–20). Recent studies using rat PC12 pheochromocytoma cells show that lead increases AP-1 DNA binding activity via a PKC-dependent pathway (21) and NF-κB activity through the activation of the MAP kinase family of kinases (22). Given the ability of lead to interfere with several signal transduction pathways and transcription factors, it is likely that lead alters gene expression in its target cells and thereby interferes with multiple cellular events in the developing brain (14, 23).

Experimental evidence points to multiple cellular targets including neurons, astroglia, and the microvasculature, at which lead may act in the developing brain (24). Astroglia are particularly important as the signals leading to expression of the blood-brain barrier phenotype appear to originate in the astrocytes and depend upon intimate astroglial-endothelial interactions (25–27). Lead has been shown to increase the permeability of the blood-brain barrier, the function of which is regulated by perivascular astrocytes (6, 26, 27). Earlier studies from this laboratory have shown that lead inhibits astroglia-induced microvessel formation *in vitro* (12). Astrocytes, therefore, appear particularly vulnerable to the toxic effects of lead (28, 29).

In this study, we have examined the effects of lead on (*a*) differential gene expression using cDNA expression microarrays and (*b*) the activity of transcription factors and related signal responsive kinases involved in the intracellular signal transduction leading to gene expression in immortalized human fetal astrocyte (SV-FHA) cultures. Our results indicate

* This work was supported by National Institute of Health Grant PO1 ES08131-02. The costs of publication of this article were defrayed in part by the payment of page charges. This article must therefore be hereby marked "*advertisement*" in accordance with 18 U.S.C. Section 1734 solely to indicate this fact.

¶ To whom correspondence should be addressed: Dept. of Neurology, The Kennedy Krieger Research Inst., 707 N. Broadway, Baltimore, MD 21205. Tel.: 410-502-8162 or -9494; Fax: 410-502-8093; E-mail: hossain@kennedykrieger.org.

[1] The abbreviations used are: PKC, protein kinase C; VEGF, vascular endothelial growth factor; AP-1, activator protein-1 complex; HIF-1, hypoxia-inducible factor 1; SV-FHA, human fetal astrocyte; DN, dominant-negative; PMA, phorbol 12-myristate 13-acetate; MAP, mitogen-activated protein; GAPDH, glyceraldehyde-3-phosphate dehydrogenase; PBS, phosphate-buffered saline; CMV, cytomegalovirus.

that among the genes induced by lead, vascular endothelial growth factor (VEGF) known also as vascular permeability factor is one of the most sensitive. Subsequent experiments determine the relative contributions of PKC, AP-1, and hypoxia-inducible factor 1 (HIF-1) regulatory pathways on lead-induced VEGF expression.

EXPERIMENTAL PROCEDURES

Materials—Dulbecco's modified Eagle's medium with 4.5 g/liter glucose and L-glutamine (Mediatech Cellgro); fetal bovine serum (Gemini Bio-Products, Inc.); lead acetate, phorbol 12-myristate 13-acetate (PMA), dimethyl sulfoxide (Me_2SO), dithiothreitol, sodium acetate, EDTA, salmon sperm DNA (Sigma); GF-109203, protease inhibitor mixture set I (Calbiochem); luciferase assay kit (Promega); poly(dI-dC) (Amersham Pharmacia Biotech); VEGF monoclonal antibody (Oncogene); Opti-MEM I, T4 polynucleotide kinase, and gentamycin (Life Technologies, Inc.); AP-1 consensus oligonucleotide (Santa Cruz Biotechnology) were purchased for the study. HIF-1 consensus sequences were custom synthesized by the DNA Synthesis Core Facility, School of Hygiene and Public Health, Johns Hopkins University. Random primed DNA labeling kit (Roche Molecular Biochemicals), [γ-^{32}P]ATP (specific activity, 3000 Ci/mmol; NEN Life Science Products), and [α-^{32}P]dCTP (specific activity, 3000 Ci/mmol) (Amersham Pharmacia Biotech) were purchased for probe labeling.

Cell Culture and Treatments—Immortalized human fetal astrocyte (SV-FHA) cells were kindly provided by Dr. Stanimirovic (Institute of Biological Sciences, National Research Council of Canada) and cultured in medium containing Dulbecco's modified Eagle's medium with 4.5 g/liter glucose and L-glutamine, 10% fetal bovine serum, and 50 μg/ml gentamycin (30). Cells were grown to 80–90% confluency prior to treatment with lead acetate, sodium acetate, and PMA. Lead acetate and sodium acetate were dissolved in sterile-distilled water and PMA in Me_2SO, and directly added to the complete medium. Final concentration of Me_2SO in the medium was 0.006% (v/v) and equal volume was used as control for PMA-exposed cells. To study the effects on VEGF expression, cells were exposed to 10 μM lead acetate for 24 h or 100 nM PMA for 6 h in complete medium unless otherwise mentioned. To study the effects on transcription factors AP-1 and HIF-1, cells were exposed to 10 μM lead acetate for 3 and 4 h, respectively, and to 100 nM PMA for 1 h prior to isolation of nuclear proteins.

cDNA Expression Microarray Assay—SV-FHAs, grown in 10-cm culture dishes to 80–90% confluency, were exposed to either 10 μM lead acetate or 10 μM sodium acetate as control. Total cellular RNA was extracted from the cells 24 h later using RNeasy isolation kit (Qiagen) according to manufacturer's protocol. Poly(A)$^+$ RNA was isolated from total cellular RNA samples and reverse transcribed in the presence of [^{32}P]dATP to generate radiolabeled cDNA probe, and purified onto Chromaspin-200 DEPC H_2O column chromatography according to the Atlas Pure RNA labeling protocol (CLONTECH). Neuroarray cDNA microarrays (CLONTECH) were hybridized with ^{32}P-labeled cDNA probes from each experimental condition according to the manufacturer's instructions. Briefly, the membranes were soaked in deionized H_2O and then blocked with sheared salmon testes DNA in ExpressHyb solution at 68 °C for 30 min. Five μl of C_ot-1 DNA was added to the labeled cDNA probe and heat denatured for 2 min followed by chilling on ice for 2 min. The cDNA probes were then added to ExpressHyb solution and the microarray blots were hybridized overnight with continuous agitation at 68 °C. The membranes were washed with Wash Solution 1 and Wash Solution 2 (supplied with kit) for 30 min each at 68 °C, and finally with 2 × SSC for 5 min at room temperature. The blots were exposed to a phosphorimaging screen at room temperature for overnight and the array image was visualized by phosphorimaging using the Bio-Image analyzer BAS 2500 (Fujifilm). Hybridized dot intensities on the microarrays were quantified using CLONTECH AtlasImage software. Normalization of the data was performed by dividing the intensity for each gene on a blot by the average intensity of all of the genes on that blot.

Northern Blot Analysis—Total cellular RNA was isolated from cells using an RNeasy isolation kit (Qiagen Inc.) as above. Northern blot analysis was performed according to the method of Sambrook and co-workers (31) with minor modifications as described previously (32). The cDNA probe for human VEGF (*Kpn*I-*Spe*I restriction fragment/582 base pairs) was labeled with [^{32}P]dCTP using a random primed DNA labeling kit (Roche Molecular Biochemicals) according to the manufacturer's instructions. Heat-denatured probe was hybridized to the membrane at 42 °C overnight (16–18 h) in 10 ml of hybridization buffer (50% formamide, 5 × SSE, 2.5 × Denhardt's solution, 0.5% SDS, and 0.2 mg/ml salmon testes DNA). The blots were washed as follows: three times in 0.1% SDS in 1 × SSC for 20 min at room temperature; and two times in the same buffer for 30 min each at 65 °C. Radioactivities corresponding to mRNA signals for VEGF were quantified by phosphorimaging using the Bio-Image analyzer BAS 2500 (Fujifilm). Membranes were stripped of probe by washing in 1 × SSC containing 0.1% SDS at 85–90 °C for 10 min and then rehybridized with cDNA probe to glyceraldehyde-3-phosphate dehydrogenase (GAPDH). Results are expressed relative to GAPDH.

Preparation of Nuclear Extracts—Nuclear extracts were prepared according to the method of Stein and co-workers (33). Briefly, cells were washed with ice-cold PBS twice and harvested by scraping in 1 ml of cold PBS. The harvested cells were centrifuged at 14,000 × *g* for 5 min. The cell pellets were resuspended in 100 μl of lysis buffer (10 mM HEPES, pH 7.9, 60 mM KCl, 1 mM EDTA, 1 mM dithiothreitol, 1 × protease inhibitor mixture, and 0.5% Nonidet P-40) and incubated on ice for 5 min. Cell lysates were centrifuged at 1,200 × *g* for 5 min at 4 °C. The nuclei recovered in the pellet were washed with 100 μl of lysis buffer without Nonidet P-40 and centrifuged at 1,200 × *g* for 5 min at 4 °C. The pellet was suspended in 100 μl of nuclear suspension buffer (250 mM Tris, pH 7.8, 60 mM KCl, 1 mM dithiothreitol, and 1 × protease inhibitor mixture) and lysed by three cycles of quick freezing in liquid nitrogen and thawing at 37 °C. The nuclear lysates were centrifuged at 14,000 × *g* for 10 min at 4 °C and the supernatants were stored at −70 °C until use for the electrophoretic mobility shift assays.

Electrophoretic Mobility Shift Assay—Electrophoretic mobility shift assay (gel-shift) was carried out to analyze the DNA binding activity of AP-1 and HIF-1 according to Ying and co-workers (34) with some modifications. Briefly, AP-1 consensus double-stranded oligonucleotides (5′-CGCTTGATGACTCAGCCGGAA-3′) were purchased from Santa Cruz Biotechnology, Inc. The sense (5′-GCCCTACGTGCT-GTCTCA-3′) and antisense (5′-TGAGACAGCACGTAGGGC-3′) HIF-1 binding sequences were synthesized by the DNA Synthesis Core Facility of Johns Hopkins University. The AP-1 consensus oligonucleotide (5 pmol) was end-labeled with [γ-^{32}P]ATP (3000 Ci/mmol; NEN Life Science Products Inc.) using T4 polynucleotide kinase (Life Technologies, Inc.) and then purified through Sephadex G-25 (Roche Molecular Biochemicals). To generate double stranded HIF-1 consensus oligonucleotide probes, the sense oligonucleotides underwent 5′ end labeling with [γ-^{32}P]ATP (NEN Life Science Products Inc.) and T4 polynucleotide kinase (Life Technologies, Inc.). The labeled sense strands were then annealed to a 10-fold excess of antisense strands by heating to 85 °C for 10 min, allowed to cool down to room temperature over a period of 2–3 h, and then purified through Sephadex G-25.

Nuclear extracts (10–15 μg) were incubated on ice for 20 min with 5 μl of a reaction buffer containing 1 μg of poly(dI-dC) (Amersham Pharmacia Biotech), 50 mM Tris-HCl (pH 7.5), 500 mM NaCl, 20% glycerol, 5 mM EDTA, 5 mM dithiothreitol in a total volume of 24 μl. One microliter of respective ^{32}P-labeled (25,000–30,000 cpm) oligonucleotide probe was added to the reaction mixture and incubated further at room temperature for 20 min. For competition studies, 100-fold excess of unlabeled oligonucleotide was added to the reaction mixture during the incubation on ice before the addition of labeled probe. DNA-protein complexes were resolved by polyacrylamide gel electrophoresis using 6% nondenaturing gel at 180 V for 3 h in 0.25 × TBE (45 mM Tris borate and 1 mM EDTA). Gels were vacuum dried and specific bands were quantified by phosphorimaging using the Bio-Imaging analyzer BAS 2500 (Fujifilm).

Immunoblot Analysis—To evaluate VEGF protein levels, cells were exposed to lead acetate (10 μM) or sodium acetate for 24 h. Cells were washed with ice-cold PBS, harvested by scraping in 1 ml of cold PBS and centrifuged at 14,000 × *g* for 5 min. Three hundred μl of RIPA buffer (1 × PBS, 1% Nonidet P-40, 0.5% sodium deoxycholate, 0.1% SDS) containing freshly added protease inhibitor mixture (Calbiochem) were added to each tube and sonicated for 10 s, centrifuged at 14,000 × *g* for 5 min and the supernatants were stored at −70 °C. One hundred μg of cell extracts were diluted to a total volume of 1 ml using 10 mM Tris (pH 7.4) and 100 mM NaCl; 30 μl of equilibrated heparin-agarose beads (Sigma) were added and the mixture rocked at 4 °C overnight as described by Ferrara and Henzel (35). The beads were pelleted at 5,000 × *g* for 1 min, washed in 400 mM NaCl and 20 mM Tris (pH 7.4), and recentrifuged at 5,000 × *g* for 1 min; the supernatant was removed and discarded. Next, 20 μl of 2 × loading buffer (20% glycerol, 100 mM Tris-HCl (pH 6.8), 4% SDS, and 0.2% bromphenol blue) were added and the slurry was heated at 100 °C for 10 min. SDS-polyacrylamide gel electrophoresis and immunoblotting were performed according to the method of Laemmli (36) with modifications. Samples (20 μl) were loaded onto a 4–20% gradient Tris glycine pre-cast gel (Novex) together

with a full range Rainbow recombinant protein molecular weight marker (Amersham Pharmacia Biotech) and run at 150 V for 1 h. Proteins were transferred electrophoretically onto a nitrocellulose membrane at constant current of 50 mA for 1 h. After blocking with 5% nonfat dried milk in 1 × Tris-buffered saline (100 mM Tris-HCl, 0.9% NaCl, pH 7.4) and 0.1% Tween-20 (TBS-T) overnight at 4 °C, the nitrocellulose membranes were incubated with VEGF monoclonal antibody (Oncogene) at 1:1000 dilution in 1 × TBS containing 0.1% bovine serum albumin for 1 h at room temperature. After washing 3 times with 1 × TBST for 10 min each, the membranes were incubated with horseradish peroxidase-conjugated protein A/G (Pierce) at 1:10,000 dilution for 1 h. Horseradish peroxidase reaction product was then visualized by enhanced chemiluminescence using an ECL Western blotting detection kit (Amersham Pharmacia Biotech) and the digitized images were quantified by densitometry (Molecular Dynamics).

Transient Expression Assays—The involvement of specific PKC isoforms was examined using dominant-negative (DN) mutants of PKC-α kindly provided by Dr. Albert Descoteaux (37) and PKC-ϵ kindly provided by Dr. P. M. Blumberg (38). These catalytically inactive mutants compete with the corresponding endogenous isoforms (37). Cells were transfected with 20 μg of either control vector DNA (pCIN-4) or the dominant-negative expression vectors DN-PKC-α or DN-PKC-ϵ by electroporation (240 V and 1050 microfarads) in a volume of 500 μl of cell suspension and replated. The involvement of AP-1 was examined by using an AP-1 luciferase reporter kindly supplied by Dr. Joseph Bressler (21) and a *jun* dominant-negative (TAM-67) plasmid expression vector kindly supplied by Dr. Michael Birrer (39). The *jun* mutant (TAM-67) lacks the transactivation domain while retaining full DNA binding capacity and inhibits AP-1 function by homodimerizing and binding to the DNA at the AP-1 sites as well as by forming heterodimers with wild type c-Fos to produce inactive heterodimers (39). Four μg of AP-1 luciferase reporter plasmid DNA along with either 20 μg of TAM-67 or control (CMV) plasmid DNA were used for electroporation as indicated above. Cells were allowed to recover for 24 h in a 5% CO_2, 95% air incubator at 37 °C. The cells were given fresh medium containing 10% serum and either lead acetate (10 μM) or sodium acetate (10 μM) as control and incubated for an additional 24 h. Alternatively, cells received PMA (100 nM) or Me_2SO (0.06% v/v) as control and were incubated for an additional 6 h.

The involvement of HIF-1 was examined by using a VEGF-luciferase reporter construct (pGL-MAP11wt) and a dominant-negative form of HIF-1α (HIF-1αDN) plasmid expression vector (pCEP/HIF-1αDN) kindly supplied by Dr. Greg Semenza (40). The pGL-MAP11wt construct includes the 5′-flanking region of human VEGF promoter containing the HIF-1 consensus DNA-binding site cloned to an SV40 promoter-luciferase transcription unit (40). The pCEP/HIF-1αDN construct encodes a form of HIF-1α lacking both the amino-terminal basic domain required for DNA-binding and the carboxyl-terminal transactivation domain. HIF-1αDN heterodimerizes with endogenous HIF-1β, generating biologically inactive heterodimers that are unable to bind DNA. Cells were co-transfected with 4 μg of pGL-MAP11wt plasmid DNA along with either 20 μg of pCEP/HIF-1αDN or control (pCEP4) plasmid DNA by electroporation as mentioned above. The total amount of plasmid DNA was adjusted to 24 μg. Twenty-four hours later cells were given fresh complete medium containing either lead acetate (10 μM) or sodium acetate (10 μM) as control and incubated for 24 h. In addition, plates containing transfected cells were incubated in 1% O_2 for 24 h at 37 °C. Cells were harvested and cell extracts were prepared using reporter lysis buffer (Promega). Luminescence was measured in 20 μl of cell extract using a luciferase assay system kit (Promega). Activity was expressed as relative light units/mg of cellular protein as determined by the Bradford method (41).

To investigate the role of AP-1 and HIF-1 in lead-induced VEGF expression, cells were electroporated with either 20 μg of TAM-67 or control (CMV) plasmid DNA and 20 μg of pCEP/HIF-1αDN or control (pCEP4) control plasmid DNA, respectively. Transfected cells were exposed to either lead or sodium acetate as indicated above. Total cellular RNA was extracted and VEGF and GAPDH levels were measured by Northern blot analysis as described above.

Statistical Analysis—Comparisons involving multiple groups were done by ANOVA followed by Bonferroni/Dunn post-hoc test. Comparison between any two groups was done by two-tailed Student's *t* test. An overall level of significance of 0.01 was used to determine differences.

RESULTS

Lead Induces Differential Gene Expression in SV-FHAs—cDNA expression microarray analyses were performed to identify lead-sensitive genes in SV-FHA cells. Poly(A)$^+$ RNA was isolated from SV-FHAs exposed to either lead acetate (10 μM) or sodium acetate as control for 24 h and used for cDNA expression microarray analysis. The cDNA microarrays used contain 588 selected genes of which 131 were consistently expressed in the SV-FHAs. Among these expressed genes, 12% appeared induced following exposure to lead. Of these induced genes one of the most lead-sensitive was VEGF (Fig. 1, *A* and *B*). Subsequent quantification of spot intensities using CLONTECH AtlasImage software revealed that lead induced VEGF mRNA 3.0-fold ($p < 0.005$) compared with sodium-treated controls (Fig. 1*C*). No significant difference in VEGF expression levels was observed between sodium-treated and untreated controls (not shown).

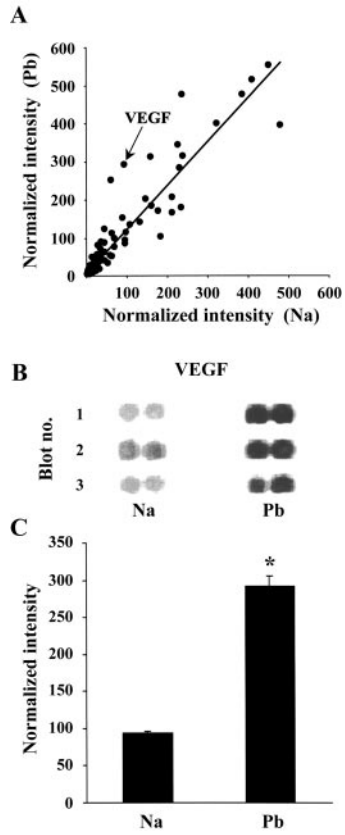

FIG. 1. **cDNA expression microarrays analysis of differential gene expression by lead in SV-FHAs.** Cells grown in normal serum (80–90% confluency) were exposed to either lead acetate (10 μM) or sodium acetate (10 μM) as control ($n = 4$). Poly(A)$^+$ RNA was isolated, and reverse transcribed to cDNA in the presence of [^{32}P]dATP as described under "Experimental Procedures." cDNA samples from each experimental condition were hybridized to 8 independent cDNA Neuroarrays (CLONTECH). *A,* gene expression values were visualized by phosphorimaging and are depicted in a scatter plot. A best fit line was generated by least squares analysis. VEGF is one of only several genes that are differentially regulated by lead acetate treatment. *B,* VEGF gene expression was identified with CLONTECH AtlasImage software based on analysis of three replicate blots from cells treated with sodium acetate (*left column*) or lead acetate (*right column*). Each gene is represented by a pair of cDNA on each blot. *C,* quantification of spot intensities shows significant up-regulation of VEGF mRNA in SV-FHAs exposed to lead relative to that of sodium or no treatment group (not shown). *, $p < 0.005$.

Lead Induces VEGF mRNA and Protein Levels in SV-FHAs—Northern blot analysis of total cellular RNA confirmed that lead induced VEGF mRNA levels in SV-FHAs compared with cells treated identically with sodium acetate. Induction of VEGF mRNA in SV-FHAs by lead was concentration and time-dependent, with maximal induction observed at 10 μM lead following 24 h of treatment (Fig. 2, *A* and *B*). Quantification of VEGF hybridization by phosphorimaging revealed that lead

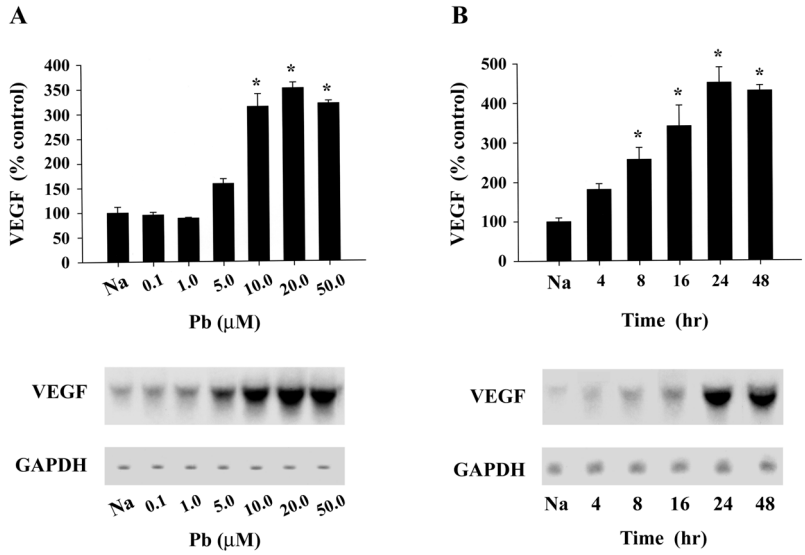

FIG. 2. **Induction of VEGF by lead is concentration- and time-dependent in SV-FHAs.** SV-FHA cells were exposed to different concentrations (0.1–50 μM) of lead acetate for 24 h (*A*) or to 10 μM lead acetate for 4–48 h (*B*). Total cellular RNA (20 μg/lane) was subjected to Northern analysis using a 582-base pair ^{32}P-labeled human VEGF cDNA probe. Blots were stripped and rehybridized with a probe to GAPDH. Specific hybridization was quantified by phosphorimaging and normalized to GAPDH. VEGF induction was maximum in response to 10 μM lead following 24 h of exposure. Data show mean ± S.E. (n = 6) of percent induction relative to sodium-treated controls. *, $p < 0.001$.

induced VEGF expression 3-fold (312 ± 25% *versus* 100 ± 9%; $p < 0.001$) compared with sodium-treated controls (Fig. 2, *A* and *B*) consistent with the magnitude of induction found in the microarray analysis. The effect of lead on VEGF protein levels was examined. Cells were exposed to 10 μM lead acetate or sodium acetate as control for 24 h and cell extracts were subjected to immunoblot analysis using anti-human VEGF monoclonal antibody. An intense VEGF immunoreactive protein band at ~46 kDa (Fig. 3) was detected. Densitometric quantification showed that VEGF protein levels were increased ~2-fold (188 ± 20% *versus* 100 ± 16%; $p < 0.01$) by lead (Fig. 3).

Involvement of PKC in VEGF Induction by Lead—The signal transduction mechanism involved in the induction of VEGF mRNA by lead was examined. Since, lead is a potent activator of PKC in other cell types, the PKC dependence of lead-induced VEGF expression in SV-FHAs was examined. In addition, PMA, a selective activator of PKC, was used as a positive control for this experiment. Treatment of SV-FHAs with lead acetate (10 μM) for 24 h and PMA (100 nM) for 6 h induced VEGF mRNA expression >2-fold (241 ± 28% *versus* 100 ± 7%; $p < 0.001$) and ~2-fold (193 ± 14% *versus* 100 ± 5%; $p < 0.001$), respectively (Fig. 4, *A* and *B*). Pretreatment of SV-FHAs with GF-109203 (2 μM), a selective cell-permeable PKC inhibitor, for 30 min completely inhibited the induction of VEGF mRNA observed following lead and PMA treatment (Fig. 4, *A* and *B*).

To further evaluate the PKC dependence of VEGF induction by lead, we used the dominant negative of the conventional PKC isoform PKC-α and the novel isoform PKC-ϵ. Cells were transfected with control vector (pCIN-4) or with either DN-PKC-α or DN-PKC-ϵ expression vectors. Twenty-four hours later, cells were exposed to either lead acetate (10 μM) or sodium acetate (10 μM) as control for an additional 24 h, or alternatively to either PMA (100 nM) or Me_2SO (0.06% v/v) as control for an additional 6 h. Northern hybridization of total cellular RNA showed >2-fold induction of VEGF mRNA (212 ± 21% *versus* 100 ± 6%; $p < 0.001$) in control- transfected cells exposed to lead acetate and ~1.7-fold induction (168 ± 13% *versus* 100 ± 8%; $p < 0.001$) in response to PMA when compared with the respective controls (Fig. 5, *A* and *B*). The induction of VEGF by lead and PMA was completely inhibited by DN-PKC-ϵ ($p < 0.001$) (Fig. 5, *A* and *B*). In contrast, DN-PKC-α had no effect on the induction of VEGF by lead (199 ± 18%) or PMA (149 ± 10%) compared with respective control-transfected cells.

Involvement of AP-1 in Lead-induced VEGF Expression—To evaluate further the downstream signaling involved in the

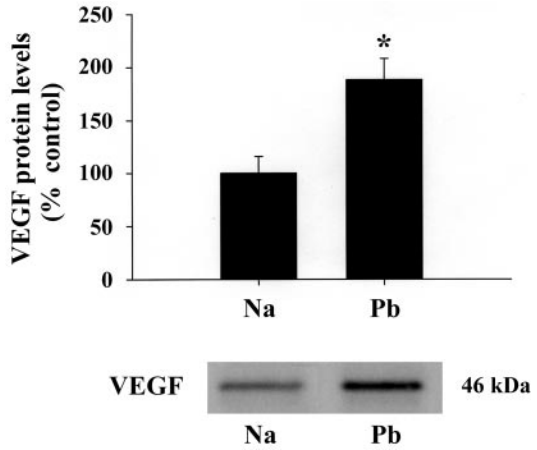

FIG. 3. **Lead induces VEGF protein levels in SV-FHAs.** Cells were exposed either to lead acetate (10 μM) or sodium acetate (10 μM) as control for 24 h. One hundred micrograms of total cellular extract were incubated with heparin-agarose beads and the heparin binding fraction subjected to immunoblot analysis using an anti-human VEGF monoclonal antibody and horseradish peroxidase-conjugated Protein A/G as described under "Experimental Procedures." Blots were exposed to ECL-film and the 46-kDa VEGF-immunoreactive protein band was quantified by densitometry. Values are shown as percent induction (mean ± S.E.; n = 6) relative to sodium-treated controls set as 100%. *, $p < 0.01$. Blots shown are from representative experiments.

mechanisms of lead's action, we examined the effects of lead on AP-1 complex in SV-FHAs. Nuclear proteins (15 μg) isolated from SV-FHAs exposed to lead acetate (10 μM) for 3 h and PMA (100 nM) for 1 h were subjected to electrophoretic mobility shift assay using ^{32}P-labeled AP-1 consensus oligonucleotide probes. Quantification by phosphorimaging revealed a 2-fold increase in AP-1 specific consensus DNA binding activity (210 ± 19% *versus* 100 ± 17%; $p < 0.01$) in lead-exposed cells relative to sodium treated controls (Fig. 6*A*). PMA stimulated a similar induction of AP-1 DNA binding activity (238 ± 2% *versus* 100 ± 5%; $p < 0.01$) (Fig. 6*A*). The AP-1 specific band disappeared when 100-fold excess of unlabeled AP-1 oligonucleotide was added to the reaction mixture (data not shown).

To determine whether lead specifically activates AP-1-dependent transcriptional activity, the ability of lead to induce AP-1-dependent luciferase reporter gene expression was examined. Cells were transfected with either 4 μg of control CMV-500 plasmid expression vector or with AP-1/luciferase reporter constructs and 24 h later exposed to lead acetate (10 μM) or

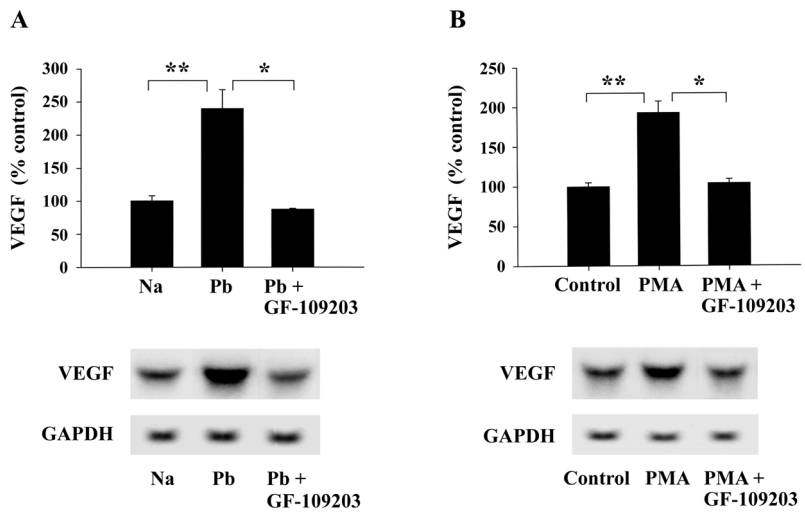

FIG. 4. **Lead induction of VEGF mRNA is PKC-dependent.** SV-FHAs cells were pretreated with PKC inhibitor GF-109203 (2 μM) for 30 min before exposure to either lead acetate (10 μM) or sodium acetate (10 μM) as control for 24 h, or before exposure to PMA (100 nM) or Me_2SO (0.006% v/v) as control for 6 h. Northern blot analysis of total cellular RNA for VEGF relative to GAPDH mRNA was performed as described under "Experimental Procedures." Pretreatment with GF-109203 completely inhibited VEGF induction by lead (*A*) or PMA (*B*). Values represent mean ± S.E. ($n = 6–10$) relative to controls (set at 100%). **, $p < 0.001$; *, $p < 0.01$. Blots shown are from representative experiments.

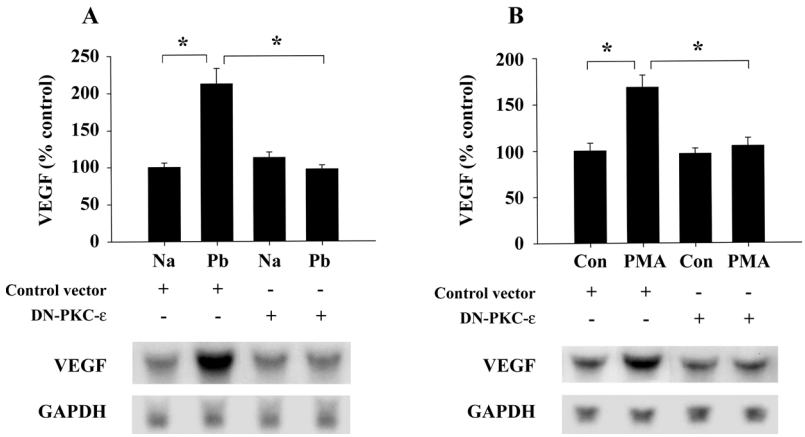

FIG. 5. **Induction of VEGF by lead is nPKC-ε-dependent.** SV-FHA cells were transfected with 20 μg of either control vector or dominant-negative PKC-ε (*DN-PKC-ε*) expression vector as described under "Experimental Procedures." Twenty-four hours later, cells were exposed to either lead acetate (10 μM) or sodium acetate (10 μM) for an additional 24 h (*A*), or to PMA (100 nM) or Me_2SO (0.006% v/v) as control for an additional 6 h (*B*). Northern blot analysis of total cellular RNA (20 μg/lane) was performed using a 582 base pairs ^{32}P-labeled human VEGF cDNA probe followed by a GAPDH probe as described under "Experimental Procedures." Specific hybridization was quantified by phosphorimaging and normalized to GAPDH. VEGF induction was completely inhibited in cells transfected with DN-PKC-ε. Values represent mean ± S.E. ($n = 6–8$) relative to controls set at 100%. *, $p < 0.001$. Blots shown are from representative experiments.

sodium acetate as control for 18–20 h. Lead increased the luciferase activity of cell extracts >2-fold (221 ± 8% *versus* 100 ± 3%; $p < 0.001$) (Fig. 6*B*). To further evaluate the AP-1 dependence of AP-1/luciferase induction by lead, cells were co-transfected with a *jun* dominant negative (TAM-67) expression vector or with control (CMV) vectors. TAM-67 lacks the transactivation domain of Jun protein and inhibits AP-1 function by binding to the consensus AP-1 sites as inactive homodimers or heterodimers. AP-1/luciferase induction by lead was inhibited by 72% ($p < 0.001$) in the TAM-67 co-transfected cells (Fig. 6*B*).

Since three AP-1 recognition sites are present in the VEGF 5′-flanking region (42), the direct involvement of AP-1 in lead-induced VEGF expression in SV-FHAs was examined. Cells were transfected with either control vector (CMV) or TAM-67 expression vector and 24 h later exposed to either lead acetate (10 μM) or sodium acetate (10 μM) as control for an additional 24 h. Northern hybridization of total cellular RNA showed >2-fold induction of VEGF mRNA (236 ± 9% *versus* 100 ± 2%; $p < 0.001$) in control CMV vector-transfected cells exposed to lead acetate compared with those exposed to sodium acetate. TAM-67 inhibited lead-induced VEGF mRNA expression by ~86% ($p < 0.001$) (Fig. 7).

Effects of Lead on HIF-1 Activation—Since the transcription factor HIF-1 is a potent activator of VEGF transcription, the effects of lead on HIF-1 DNA binding activity were also examined. Nuclear proteins isolated from SV-FHAs exposed to either lead acetate (0.1–50 μM) or sodium acetate for 0.5–6 h were subjected to electrophoretic mobility shift assay using ^{32}P-labeled oligonucleotide probes containing HIF-1 binding consensus sequences. Quantification of shifted bands by phosphorimaging showed a small but reproducible and significant increase in HIF-1 DNA binding activity in response to lead exposure. The HIF-1 specific band disappeared when 140-fold excess of unlabeled oligonucleotide probe was added to the reaction mixture (not shown). The induction of HIF-1 activity was concentration and time-dependent, with maximum induction occurring at 10 μM lead exposure for 4 h relative to the control (196 ± 28% *versus* 100 ± 7%; $p < 0.001$) (Fig. 8, *A* and *B*).

Because the VEGF induction by lead was found to be PKC-dependent, we examined the role of PKC in HIF-1 induction using the specific PKC activator PMA and the selective PKC inhibitor GF-109203. Electrophoretic mobility shift assay showed that PMA (100 nM) induced HIF-1 binding activity ~2-fold (196 ± 34% *versus* 100 ± 12%; $p = 0.01$) with maximum activity occurring at 1 h of exposure. Cells were pretreated with GF-109203 (2 μM) for 30 min prior to lead (10 μM) or PMA (100 nM) exposure for 4 and 1 h, respectively. Lead induction of HIF-1 DNA binding activity was inhibited in cells

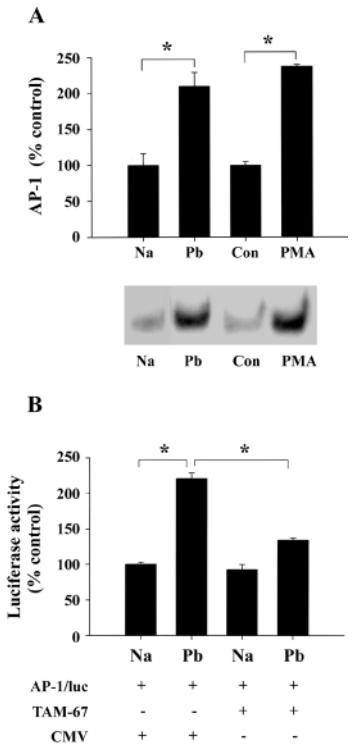

FIG. 6. **Lead activates AP-1 DNA binding activity and AP-1-dependent reporter gene expression.** *A,* nuclear protein was isolated from SV-FHAs exposed to either lead acetate (10 μM) or sodium acetate as control for 3 h, or to either PMA (100 nM) or Me_2SO (0.006% v/v) as control for 1 h. Electrophoretic mobility shift assays (15 μg of protein/lane) were performed using ^{32}P-labeled AP-1 consensus oligonucleotide probes as described under "Experimental Procedures." AP-1 DNA binding activity increased >2-fold in cells exposed to either lead or PMA. *B*, cells were co-transfected with 4 μg of AP-1/luciferase reporter constructs along with either 20 μg of the c-*jun* dominant-negative TAM-67 or control (CMV) plasmid DNA. After 24 h, cells were exposed to either lead acetate (10 μM) or sodium acetate as control for an additional 18–20 h. Luciferase expression was quantified in 20 μl of cell extracts by measuring luminescence normalized to total protein as described under "Experimental Procedures." Data represents mean ± S.E. relative to sodium-treated controls (set at 100%). *, $p < 0.01$. Blots shown are from representative experiments.

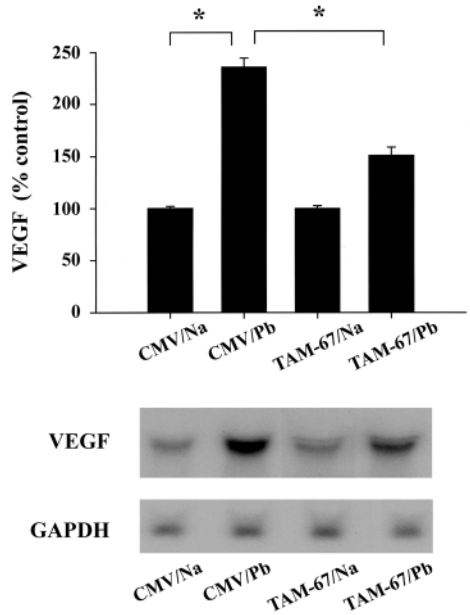

FIG. 7. **Induction of VEGF by lead is AP-1-dependent.** Cells were transfected with either 20 μg of control (CMV) or c-*jun* dominant-negative TAM-67 expression vectors and 24 h later exposed to either lead acetate (10 μM) or sodium acetate (10 μM) as control for an additional 24 h. Total cellular RNA (20 μg/lane) was subjected to Northern analysis using a 582-base pair ^{32}P-labeled human VEGF cDNA probe followed by a GAPDH probe as described under "Experimental Procedures." Specific hybridization was quantified by phosphorimaging and normalized to GAPDH. Expression of VEGF mRNA was significantly inhibited in cells transfected with TAM-67. Data represents mean ± S.E. ($n = 6–8$) relative to sodium-treated controls (set at 100%). *, $p < 0.001$. Blots shown are from representative experiments.

pretreated with the GF-109203 both in the case of lead and PMA (Fig. 9, *A* and *B*).

Involvement of HIF-1 in Transcriptional Activation of VEGF—To determine whether the increase in HIF-1 DNA binding activity in lead-treated cells reflects a change in HIF-1 regulated transcriptional events, cells were co-transfected with 4 μg of a VEGF-luciferase expression vector (p-GL/MAP11wt) along with either 20 μg of a HIF-1α dominant-negative expression vector (pCEP/HIF-1αDN) or its control pCEP4 plasmid DNA. The total amount of plasmid DNA transfected was held constant at 24 μg. The VEGF/luciferase reporter construct includes the 5′-flanking region of human VEGF promoter containing the HIF-1 consensus DNA-binding site (40). The pCEP/HIF-1αDN construct encodes a form of HIF-1α lacking both the amino-terminal basic domain required for DNA binding and the carboxyl-terminal transactivation domain. HIF-1αDN heterodimerizes with HIF-1β generating biologically inactive heterodimers and inhibits HIF-1-regulated reporter gene expression. Twenty-four hours after transfection, cells were exposed to either lead acetate (10 μM) or sodium acetate for an additional 18–20 h. There was no significant difference in luciferase activity in cells exposed to lead or sodium acetate (Fig. 10*A*). As a positive control, transfected cells were exposed to hypoxia (1% O_2 at 37 °C) for 24 h. Hypoxia increased luciferase activity >8-fold (867 ± 40% *versus* 100 ± 6%; $p < 0.001$) relative to normoxic cells co-transfected with p-GL/MAP11wt and pCEP4 plasmid DNA. In the presence of pCEP/HIF-1αDN, hypoxia-induced luciferase activity was inhibited by 60% ($p < 0.001$) (Fig. 10*A*) demonstrating that pCEP/HIF-1αDN effectively inhibits HIF-1-dependent reporter gene expression under these experimental conditions.

The potential role of HIF-1 in the transcriptional activation of VEGF by lead was similarly examined using the dominant-negative HIF-1αDN. SV-FHAs were transfected with either the control pCEP4 vector DNA or pCEP/HIF-1αDN (20 μg) expression vectors. Twenty-four hours later, cells were exposed to lead acetate (10 μM) or sodium acetate as control for an additional 24 h. Northern hybridization of total RNA revealed 3-fold induction of VEGF mRNA by lead (306 ± 22% *versus* 99 ± 4%; $p < 0.001$ relative to control) in cells transfected with control pCEP4 plasmid. pCEP/HIF-1αDN had no effect on the induction of VEGF mRNA by lead (Fig. 10*B*).

DISCUSSION

Lead is a widespread environmental toxicant whose developmental neurotoxicity remains a major medical issue. There is growing evidence that lead can directly alter cellular physiology at multiple levels which include interference with ion channels and activation of second messengers, in particular calcium-dependent messengers, that ultimately affect transcription factors and gene expression. This report demonstrates that lead alters the expression of human fetal astrocyte genes and defines the second messenger and transcription factors involved in the induction of one of these genes, VEGF/vascular permeability factor. VEGF induction was observed in this study in response to low micromolar total lead in 10% serum-containing medium, a condition in which almost all lead will be chelated by serum proteins. Actual measurements of free-lead concentrations in serum-containing cell culture medium by

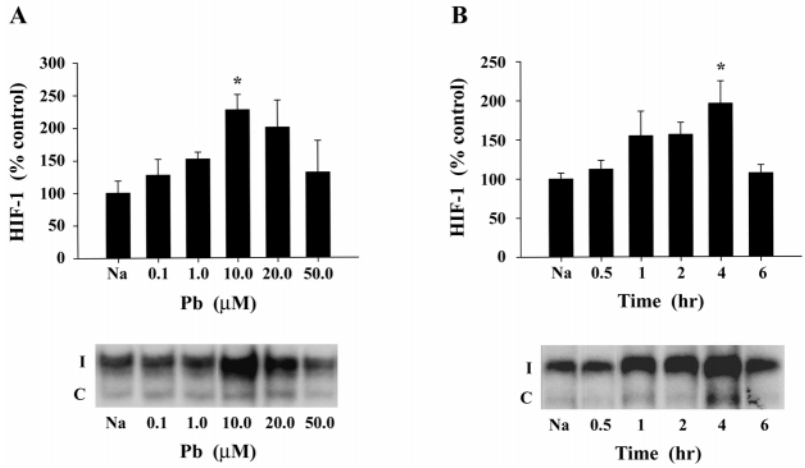

FIG. 8. **Effects of lead on the HIF-1 DNA binding activity.** *A,* cells were exposed to either varying concentrations of lead acetate (0.1–50 μM) or sodium acetate as control for 4 h. Nuclear proteins (15 μg/lane) were analyzed by electrophoretic mobility shift assay using ^{32}P-labeled oligonucleotide probes containing HIF-1 binding consensus sequences as described under "Experimental Procedures." *B,* cells were exposed to either lead acetate (10 μM) or sodium acetate as control for 0.5–6 h. HIF-1 DNA binding activity was determined as above. Maximum activity was observed at 10 μM concentration following 4 h of exposure. Data represent mean ± S.E. relative to controls (set at 100%). *, $p < 0.01$. Blots shown are from representative experiments.

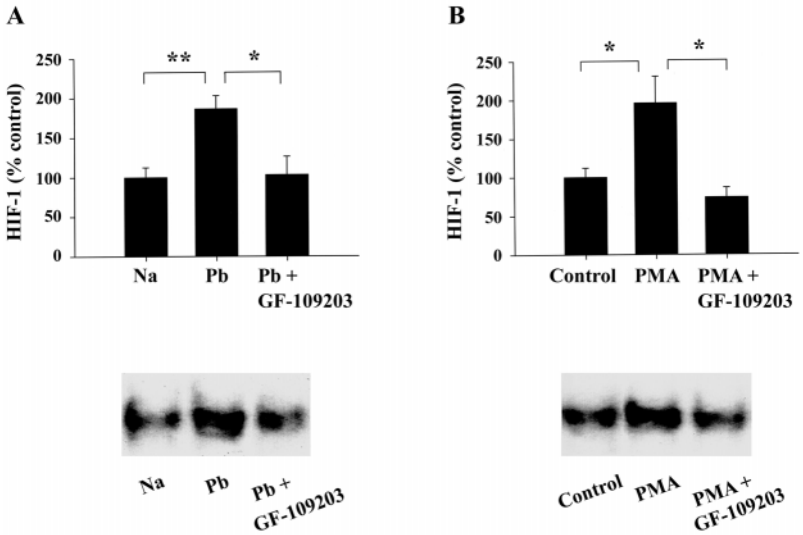

FIG. 9. **Involvement of PKC in HIF-1 induction by lead.** Cells were pretreated with GF-109203 (2 μM) for 30 min prior to treatment with either lead acetate (10 μM) or sodium acetate for 4 h (*A*), or with either PMA (100 nM) or Me_2SO (0.006% v/v) as control for 1 h (*B*). Nuclear proteins were analyzed by electrophoretic mobility shift assay. Induction of HIF-1 DNA binding activity by either lead or PMA was inhibited in cells pretreated with the GF-109203. Data represents mean ± S.E. relative to controls (set at 100%). *, $p < 0.01$; **, $p < 0.001$. Blots shown are from representative experiments.

Audesirk and co-workers (43), predicts that the free lead levels under our experimental conditions were in the nanomolar range, a concentration that is relevant to human toxicity (5, 16, 24). To our knowledge this is the first application of cDNA microarray analysis to questions of lead toxicity and the first detailed dissection of the effect of lead on cell signaling and transcription factor function in cells derived from the human central nervous system.

It has been established previously in rodent cells and purified protein preparations that lead alters a number of diverse calcium-sensitive processes. These include inhibition of calcium-channels, activation of calmodulin, and activation of PKC (11, 13, 44). Of these, PKC appears to be particularly relevant. The PKC family comprises more than 10 isoforms categorized into three structurally related groups: conventional PKCs (cPKCs: α, β, and γ) are regulated by calcium and diacylglycerol or phorbol ester; novel PKCs (nPKCs: δ, θ, η, and ϵ) are sensitive to diacylglycerol and phorbol ester but are calcium-independent; and atypical PKCs (aPKCs: ζ, μ, and ι) are insensitive to calcium, diacylglycerol, and phorbol ester (45). Activation of both calcium-dependent and calcium-independent PKC isoforms by lead has been described in rodent and bovine cells such as glial, endothelial, and PC12 pheochromocytoma cell lines (12, 46, 47). It has been proposed that lead alters PKC function by interacting with a high affinity site within the NH_2-terminal regulatory domain either at the calcium activation site or cysteine-rich zinc-finger-like binding site (11, 15, 48). A role for PKC in the induction of VEGF by lead described in this report is supported by complementary approaches. The PKC activator PMA induced VEGF mRNA levels in the human fetal astrocyte cell line and, furthermore, both lead and PMA induction of VEGF were blocked by the selective PKC inhibitor GF-109203. Since GF-109203 inhibits both calcium-dependent and calcium-independent PKC isoforms, the specific isoforms involved in the VEGF response were further examined using dominant-negative mutants of representative calcium-dependent conventional PKC-α and calcium-independent novel PKC-ϵ isoforms. Such catalytically inactive dominant-negative molecules act by competing with the corresponding endogenous isoforms (37). The selective involvement of PKC-ϵ, but not the PKC-α, in VEGF induction by lead and PMA was directly demonstrated through its inhibition by DN-PKC-ϵ. These results clearly implicate a specific role of PKC-ϵ in this lead response in SV-FHAs. Similarly, PKC-ϵ has been found to play a role in the induction of immediate early gene expression in the rat PC12 cells (47). The potential involvement of other PKC isoforms in response of human astrocytes to lead is currently under investigation.

PKC activation induces the transcription of immediate early response genes such as c-*jun* and c-*fos* that comprise the AP-1 transcription factor through either Jun homodimerization or Jun/Fos heterodimerization (18–20). The present study used multiple approaches to show that lead alters AP-1 activity in SV-FHAs. Increased AP-1 DNA binding activity in nuclear proteins isolated from lead-treated cells was shown by electrophoretic mobility shift assay similar to that reported in the rat

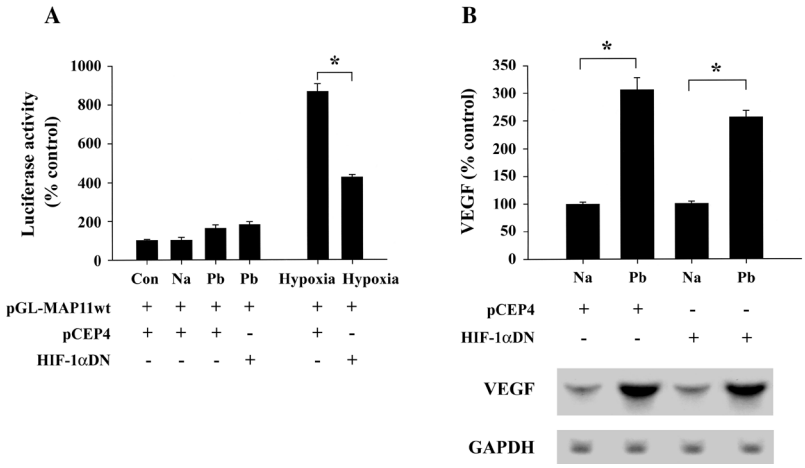

FIG. 10. **Lead does not induce HIF-1-dependent transcriptional activity.** *A,* cells were co-transfected with 4 μg of a VEGF-luciferase reporter construct (pGL-MAP11wt) along with either 20 μg of a HIF-1α dominant-negative expression vector (pCEP/HIF-1αDN) or its control plasmid DNA (pCEP4). The pGL-MAP11wt construct includes the 5′-flanking region of the human VEGF promoter containing the HIF-1 consensus DNA-binding site as described under "Experimental Procedures." Total amount of transfected plasmid DNA was held constant at 24 μg. Twenty-four hours after transfection, cells were exposed either to lead acetate (10 μM) or sodium acetate (10 μM) as control, or to hypoxia (1% O_2 at 37 °C) as positive control for additional 24 h. Luciferase expression was quantified in 20 μl of cell extracts by measuring luminescence normalized to total proteins. Hypoxia-induced luciferase expression is inhibited by HIF-1α dominant-negative. *B,* cells were transfected with 20 μg of either pCEP/HIF-1αDN or control plasmid vector pCEP4, and 24 h later exposed to either 10 μM lead acetate or sodium acetate as control for additional 24 h. Total cellular RNA (20 μg /lane) was subjected to Northern analysis. Specific VEGF hybridization was quantified by phosphorimaging and normalized to GAPDH as described under "Experimental Procedures." Northern data revealed no inhibition of lead-induced VEGF expression by HIF-1α dominant-negative. Data represents mean ± S.E. (n = 6–8) relative to controls (set at 100%). *, $p < 0.001$. Blots shown are from representative experiments.

PC12 cell line (21). The functional relevance of this *in vitro* assay is demonstrated by the ability of lead to induce AP-1-dependent reporter gene expression in transiently transfected SV-FHA cells and by the inhibition of this lead-induced transcriptional response by the c-*jun* dominant-negative TAM-67 (39). Finally, the physiological relevance of this lead-induced AP-1 activation in SV-FHAs was examined. Given the presence of AP-1 consensus binding sites in the 5′-flanking region of VEGF (40, 42), we investigated the role of AP-1 in VEGF expression in response to lead. The involvement of AP-1 in the lead-mediated induction of VEGF mRNA was directly demonstrated through its inhibition by TAM-67. These results clearly demonstrate the requirement for AP-1 transcription factors for lead-induced VEGF expression.

Due to the prominent role of HIF-1 in the regulation of VEGF expression, a similar multifaceted approach was taken to examine the effects of lead on HIF-1 and its potential role in VEGF induction by lead. HIF-1 is a heterodimeric transcription factor consisting of HIF-1α and HIF-1β subunits and is essential for the activation of genes mediating responses to hypoxia (40, 49). HIF-1 mediated transcriptional activity depends upon both the post-translational stabilization of HIF-1α, probably through selective protection from ubiquitin-dependent proteolysis, and the increased activity of HIF-1α transactivating domains which may together exert synergistic effects (50). Hypoxia sensing mechanisms upstream to HIF-1 activation are not well defined in astrocytic cells but may mirror a mechanism partially characterized in type I cells of the carotid body and in PC12 cells that involve increased cytoplasmic calcium from calcium channel activation, PKC, and heme metabolism. The ability of lead to alter calcium-mediated processes (9, 10), to activate PKC (11–13), and to interfere with heme biosynthesis (51) suggested a potential interface with HIF-1 function. While our gel-shift assay results indicate that exposing cells to either lead or the PKC-agonist PMA enhances HIF-1 binding to its DNA consensus sequence ~2-fold, no downstream HIF-1-dependent VEGF-specific transcriptional events could be identified using two complementary methods. Neither lead nor PMA enhanced reporter gene expression under transcriptional control of HIF-1 binding sequences derived from the 5′-flanking region of the human VEGF gene in intact SV-FHAs. In addition, VEGF induction by lead was not affected by the HIF-1α dominant-negative under conditions that inhibited a much stronger hypoxia-induced VEGF response. These disparate results might be explained by a consideration of the different magnitudes of HIF-1 induction seen in response to lead and hypoxia. The magnitude of increased HIF-1 binding activity in nuclear proteins derived from lead-treated cells while statistically significant was small and possibly inadequate to generate a transcriptional response. Alternatively, lead may generate HIF-1 heterodimers comprised of β-like Per-ARNT-Sim (PAS) family members such as neural specific nPAS-2 (52) that are less effective in transcriptional activation than heterodimers induced by hypoxia (53). The possibility that lead might modulate HIF-1-dependent hypoxic responses has not been addressed.

VEGF is a dimeric secretory protein containing an amino terminus secretory sequence (42, 54) and exerts its action via high-affinity binding to phosphotyrosine kinase receptors Flt-1 and Flk-1 (55, 56). Compelling evidence indicates that VEGF is a fundamental regulator of physiological and pathological angiogenesis (35, 54). VEGF is crucially involved in mediating vascular changes following neuronal injury (57). Overexpression of VEGF can contribute to progression of several disorders such as intracerebral hemorrhage (58), development of brain edema (59), and disruption of blood-brain barrier, pathological processes seen in acute lead toxicity (6, 7). In addition neurons have recently been found to express high-affinity VEGF receptors and thereby might be influenced directly to VEGF disregulation (60).

In conclusion, this is the first evidence that lead induces the expression of a growth factor (*i.e.* VEGF). This is also the first dissection of the second messenger pathways and transcription factors that mediate the effects of lead on gene expression in human central nervous system cells. The potential roles of VEGF and other astrocytic gene products in the spectrum of the vascular and cognitive symptoms associated with lead toxicity warrants further investigation.

Acknowledgment—We thank Angela T. Williams for assistance in the preparation of this manuscript.

REFERENCES

1. Center for Disease Control (1991) *Preventing Lead Poisoning in Young Children*, CDC, Atlanta, GA
2. Agency for Toxic Substances and Disease Registry (1992) in *Toxicological Profile for Lead*, pp. 105, U. S. Department of Health and Human Services, Public Health Service, Agency for Toxic Substances and Disease Registry, Atlanta, GA
3. WHO (1995) in *Environmental Health Criteria*, pp. 165, World Health Organization, Geneva
4. Nriagu, J. O. (1996) *Science* **272,** 223–224
5. Winneke, G., Lilienthal, H., and Kramer, U. (1996) *Arch. Toxicol. Suppl.* **18,** 57–70
6. Clasen, R. A., Hartmann, J. F., Starr, A. J., Coogan, P. S., Pandolfi, S., Laing, I., Becker, R., and Hass, G. M. (1973) *Am. J. Pathol.* **74,** 215–240
7. Goldstein, G. W., Asbury, A. K., and Diamond, I. (1974) *Arch. Neurol.* **31,** 382–389
8. Press, M. F. (1977) *J. Neuropathol. Exp. Neurol.* **36,** 169–193
9. Goldstein, G. W., and Ar, D. (1983) *Life Sci.* **33,** 1001–1006
10. Habermann, E., Crowell, K., and Janicki, P. (1983) *Arch. Toxicol.* **54,** 61–70
11. Markovac, J., and Goldstein, G. W. (1988) *Nature* **334,** 71–73
12. Laterra, J., Bressler, J. P., Indurti, R. R., Belloni-Olivi, L., and Goldstein, G. W. (1992) *Proc. Natl. Acad. Sci. U. S. A.* **89,** 10748–10752
13. Long, G. J., Rosen, J. F., and Schanne, F. A. (1994) *J. Biol. Chem.* **269,** 834–837
14. Kikkawa, U., Kishimoto, A., and Nishizuka, Y. (1989) *Annu. Rev. Biochem.* **58,** 31–44
15. Burns, D. J., and Bell, R. M. (1991) *J. Biol. Chem.* **266,** 18330–18338
16. Bressler, J., Kim, K. A., Chakraborti, T., and Goldstein, G. (1999) *Neurochem. Res.* **24,** 595–600
17. Kim, K., Annadata, M., Goldstein, G. W., and Bressler, J. P. (1997) *Intl. J. Dev. Neurosci.* **15,** 175–182
18. Halazonetis, T. D., Georgopoulos, K., Greenberg, M. E., and Leder, P. (1988) *Cell* **55,** 917–924
19. Sheng, M., and Greenberg, M. E. (1990) *Neuron* **4,** 477–485
20. Karin, M., Liu, Z., and Zandi, E. (1997) *Curr. Opin. Cell Biol.* **9,** 240–246
21. Chakraborti, T., Kim, K. A., Goldstein, G. G., and Bressler, J. P. (1999) *J. Neurochem.* **73,** 187–194
22. Ramesh, G. T., Manna, S. K., Aggarwal, B. B., and Jadhav, A. L. (1999) *Toxicol. Appl. Pharmacol.* **155,** 280–286
23. Singh, A. K. (1995) *Neurotoxicology* **14,** 417–428
24. Goldstein, G. W. (1991) in *Human Lead Exposure* (Needleman, H. L., ed) pp. 125–135, CRC, Boca Ratan, FL
25. Ling, T. L., Mitrofanis, J., and Stone, J. (1989) *J. Comp. Neurol.* **286,** 345–352
26. Bradbury, M. W. (1984) *Fed. Proc.* **43,** 186–190
27. Goldstein, G. W. (1988) *Ann. N. Y. Acad. Sci.* **25,** 31–39
28. Gebhart, A. M., and Goldstein, G. W. (1988) *Toxicol. Appl. Pharmacol.* **94,** 191–206
29. Holtzman, D., Olson, J. E., DeVries, C., and Bensch, K. (1987) *Toxicol. Appl. Pharmacol.* **89,** 211–225
30. Muruganandam, A., Herx, L. M., Monette, R., Durkin, J. P., and Stanimirovic, D. B. (1997) *FASEB J.* **11,** 1187–1197
31. Sambrook, J., Fritsch, E. F., and Maniatis, T. (1996) in *Molecular Cloning*, pp. 7.35–7.39, Cold Spring Harbor Press, Cold Spring Harbor, NY
32. Hossain, M. A., Fielding, K. E., Trescher, W. H., Ho, T., Wilson, M. A., and Laterra, J. (1998) *Eur. J. Neurosci.* **10,** 2490–2499
33. Stein, B., Rahmsdorf, H. J., Steffen, A. L. M., and Herrlich, P. (1989) *Mol. Cell. Biol.* **9,** 5169–5181
34. Ying, Z., Reisman, D., and Buggy, J. (1996) *Mol. Brain Res.* **39,** 109–116
35. Ferrara, N., and Henzel, W. J. (1989) *Biochem. Biophys. Res. Commun.* **161,** 851–858
36. Laemmli, U. K. (1970) *Nature* **227,** 680–685
37. St-Denis, A., Chano, F., Tremblay, P., St-Pierre, Y., and Descoteaux, A. (1998) *J. Biol. Chem.* **273,** 32787–32792
38. Brodie, C., Bogi, K., Acs, P., Lazarovici, P., Petrovics, G., Anderson, W. B., and Blumberg, P. M. (1999) *Cell Growth Differ.* **10,** 183–191
39. Brown, P. H., Chen, T. K., and Birrer, M. J. (1994) *Oncogene* **9,** 791–799
40. Forsythe, J. A., Jiang, B. H., Iyer, N. V., Agani, F., Leung, S. W., Koos, R. D., and Semenza, G. L. (1996) *Mol. Cell. Biol.* **16,** 4604–4613
41. Bradford, M. M. (1976) *Anal. Biochem.* **72,** 248–254
42. Tischer, E., Mitchell, R., Hartman, T., Silva, M., Gospodarowicz, D., Fiddes, J. C., and Abraham, J. A. (1991) *J. Biol. Chem.* **266,** 11947–11954
43. Audesirk, G., Shugarts, D., Nelson, G., and Przekwas, J. (1989) *In Vitro Cell Dev. Biol.* **25,** 1121–1128
44. Bressler, J. P., and Goldstein, G. W. (1991) *Biochem. Pharmacol.* **41,** 479–484
45. Kazanietz, M. G., and Blumberg, P. M. (1996) in *Cellular and Molecular Pathogenesis*, pp. 389–402, Lippincott-Raven, Philadelphia
46. Belloni-Olivi, L., Annadata, M., Goldstein, G. W., and Bressler, J. P. (1996) *Biochem. J.* **315,** 401–406
47. Kim, K. A., Chakraborti, T., Goldstein, G. W., and Bressler, J. P. (2000) *J. Neurochem.* **74,** 1140–1146
48. Tomsig, J. L., and Suszkiw, J. B. (1995) *J. Neurochem.* **64,** 2667–2673
49. Wang, G. L., and Semenza, G. L. (1995) *J. Biol. Chem.* **270,** 1230–1237
50. Jiang, B. H., Zheng, J. Z., Leung, S. W., Roe, R., and Semenza, G. L. (1997) *J. Biol. Chem.* **272,** 19253–19260
51. Lubran, M. M. (1980) *Ann. Clin. Lab. Sci.* **10,** 402–13
52. Zhou, Y. D., Barnard, M., Tian, H., Li, X., Ring, H. Z., Francke, U., Shelton, J., Richardson, J., Russell, D. W., and McKnight, S. L. (1997) *Proc. Natl. Acad. Sci. U. S. A.* **94,** 713–718
53. Halterman, M. W., Miller, C. C., and Federoff, H. J. (1999) *J. Neurosci.* **19,** 6818–6824
54. Leung, D. W., Cachianes, G., Kuang, W. J., Goeddel, D. V., and Ferrara, N. (1989) *Science* **246,** 1306–1309
55. De Vries, C., Escobedo, J. A., Ueno, H., Houck, K., Ferrara, N., and Williams, L. T. (1992) *Science* **255,** 989–991
56. Quinn, T. P., Peters, K. G., De Vries, C., Ferrara, N., and Williams, L. T. (1993) *Proc. Natl. Acad. Sci. U. S. A.* **90,** 7533–7537
57. Bartholdi, D., Rubin, B. P., and Schwab, M. E. (1997) *Eur. J. Neurosci.* **9,** 2549–2560
58. Cheng, S. Y., Nagane, M., Huang, H. S., and Cavenee, W. K. (1997) *Proc. Natl. Acad. Sci. U. S. A.* **94,** 12081–12087
59. Bates, D. O., and Curry, F. E. (1996) *Am. J. Physiol.* **271,** H2520–2528
60. Sondell, M., Lundborg, G., and Kanje, M. (1999) *J. Neurosci.* **19,** 5731–5740